Weak coupling magnetism in $Ce_4Pt_{12}Sn_{25}$: a small exchange limit in the Doniach phase diagram

2010 J. Phys.: Condens. Matter 22 065601

(http://iopscience.iop.org/0953-8984/22/6/065601)

J. Phys.: Condens. Matter **22** (2010) 065601 (5pp) doi:10.1088/0953-8984/22/6/065601

Weak coupling magnetism in $Ce_4Pt_{12}Sn_{25}$: a small exchange limit in the Doniach phase diagram

Han-Oh Lee[1], Nobuyuki Kurita[1], Pei-chun Ho[2], Cathie L Condron[3], Peter Klavins[4], Susan M Kauzlarich[3], M B Maple[5], R Movshovich[1], E D Bauer[1], J D Thompson[1] and Z Fisk[1,6]

[1] Los Alamos National Laboratory, Los Alamos, NM 87545, USA
[2] Department of Physics, California State University, Fresno, CA 93740, USA
[3] Department of Chemistry, University of California, Davis, CA 95616, USA
[4] Department of Physics, University of California, Davis, CA 95616, USA
[5] Department of Physics, University of California, San Diego, La Jolla, CA 92093, USA
[6] Department of Physics and Astronomy, University of California, Irvine, CA 92697, USA

Received 30 October 2009, in final form 13 December 2009
Published 27 January 2010
Online at stacks.iop.org/JPhysCM/22/065601

Abstract
Magnetic susceptibility, magnetization, specific heat, and electrical resistivity studies on single crystals of $Ce_4Pt_{12}Sn_{25}$ reveal an antiferromagnetic transition at $T_N = 0.19$ K, which develops from a paramagnetic state with a very large specific heat coefficient (C/T) of 14 J mol^{-1} K^{-2}-Ce just above T_N. On the basis of its crystal structure and these measurements, we argue that a weak magnetic exchange interaction in $Ce_4Pt_{12}Sn_{25}$ is responsible for its low ordering temperature and a negligible Kondo-derived contribution to physical properties above T_N. The anomalous enhancement of specific heat above T_N is suggested to be related, in part, to weak geometric frustration of f-moments in this compound.

(Some figures in this article are in colour only in the electronic version)

1. Introduction

Kondo-lattice systems have attracted interest due to the unusual and widely varying ground states that emerge from strong electronic correlations [1, 2]. The primary interactions in these systems are the Kondo coupling between a local moment and itinerant electrons [3] and the itinerant-electron mediated Ruderman–Kittel–Kasuya–Yosida (RKKY) interaction [4] between localized moments, both of which depend on the magnetic exchange J between local spin and conduction electrons. The Kondo interaction, which grows exponentially with J, produces a non-magnetic singlet at sufficiently low temperatures, whereas, the RKKY interaction, which depends quadratically on J, promotes long-range magnetic order. By their natures, these two interactions compete with each other. Doniach has considered this competition as a function of J for a one-dimensional Kondo necklace [5]. When J is small, the intersite RKKY interaction dominates and the system orders magnetically (either antiferromagnetic or ferromagnetic ground state); but when J is larger, magnetic order is suppressed and the system eventually enters a paramagnetic phase once Kondo-screening of the moments dominates. Between these extreme limits of J, the magnetic ordering temperature approaches zero, where non-Fermi-liquid behaviors and unconventional superconductivity often emerge [6]. Despite a variety of the ground states having been studied and a large number of different compounds having been reported to be Kondo-lattice systems, there have been few examples of the very small-J limit. Here we report on the Kondo-lattice system $Ce_4Pt_{12}Sn_{25}$ that shows characteristics of weak Kondo and RKKY interactions: an antiferromagnetic transition at ~0.19 K, which is an unusually low temperature for a Ce-based Kondo lattice, and a negligible Kondo-derived contribution to specific heat or electrical resistivity above T_N.

2. Experimental details

Single crystals of $Ce_4Pt_{12}Sn_{25}$ were grown using excess Sn as a flux. The constituent elements were placed in an

alumina crucible and sealed in an evacuated quartz tube. The ampule was then heated to 1180 °C, followed by slow cooling down to 500 °C before spinning the quartz tube to separate the crystals from molten flux. Using a similar procedure, we also synthesized single crystals of the non-magnetic analog $La_4Pt_{12}Sn_{25}$ in order to compare it with $Ce_4Pt_{12}Sn_{25}$. Single crystal x-ray diffraction patterns were collected at room temperature using an R3m/V Siemens diffractometer, with Mo K_α radiation at $\lambda = 0.710\,73$ Å and with a graphite monochromator and a modified Enraf-Nonius low-temperature apparatus. The ψ-scan method was used to perform an empirical absorption correction. The structure was identified by direct methods and refined by the full-matrix least-squares method on F^2 (SHELXTL-97, Sheldrick 1990). Temperature-dependent dc magnetic susceptibility and field-dependent magnetization were measured with a Quantum Design MPMS. A standard lock-in technique was used to measure ac susceptibility from 17 mK to 2 K. Heat capacity, determined by a relaxation-time technique and heat pulse measurement, and four-probe electrical resistivity were measured to 0.35 K in a Quantum Design PPMS and to 70 mK in a dilution refrigerator.

3. Results and discussion

Except for its crystal structure, first reported by Chafik *et al* [7], no physical properties of $Ce_4Pt_{12}Sn_{25}$ are known. Analysis of our x-ray diffraction data verifies that single crystals of $Ce_4Pt_{12}Sn_{25}$ form in a complex cubic structure with space group $Im\bar{3}$, as found by Chafik *et al*, and no residual peaks in the refinement were present. Although the structure is cubic, Ce atoms occupy sites with three-fold point symmetry, which is expected to split the six-fold degenerate ground state of Ce^{3+} into three crystal-field doublets. As shown in figure 1, Ce sites, separated by a large distance of 6.14 Å, are surrounded by a cage of 6-Pt nearest neighbors (at ∼3.34 Å) and 12-Sn atoms (six at Sn2 and six at Sn3 positions), forming edge-sharing hexacapped deformed cuboctahedra. At a Ce–Sn3 separation of ∼3.44 Å, the six Sn3 sites are comparable to Pt atoms in their distance from Ce. As shown by Chafik *et al*, thermal vibrations of the Sn3 atoms are large and anisotropic, giving rise to a static deformation with two statistically significant sites called Sn3 and Sn3′, each about 50% deficient. This crystal structure has the same space group as filled skutterudites; however, the rare-earth ion in skutterudites sits at the 2a site, forming a body-centered cubic environment, but Ce in $Ce_4Pt_{12}Sn_{25}$ is located at the 8c site that is occupied by transition-metal atoms in the skutterudite structure. As a result, the Ce site in CeT_4Pn_{12} (T = Fe, Ru, Os; Pn = P, As, Sb) skutterudites is surrounded by 12 Pn icosahedral cages that are not shared by any other Ce atoms [8]. In $Ce_4Pt_{12}Sn_{25}$, 6-Pt and 12-Sn hexacapped-cuboctahedral cages are shared by other Ce atoms. Furthermore, the distance from Sn2 to Ce in $Ce_4Pt_{12}Sn_{25}$ is 3.776 Å, a rather large distance not favorable for strong f–p hybridization. Thus, the number of effective atoms around Ce is six per each Ce atom. Though the Ce–Ce distance in skutterudites is somewhat larger (∼7–8 Å) than in $Ce_4Pt_{12}Sn_{25}$, the smaller number of

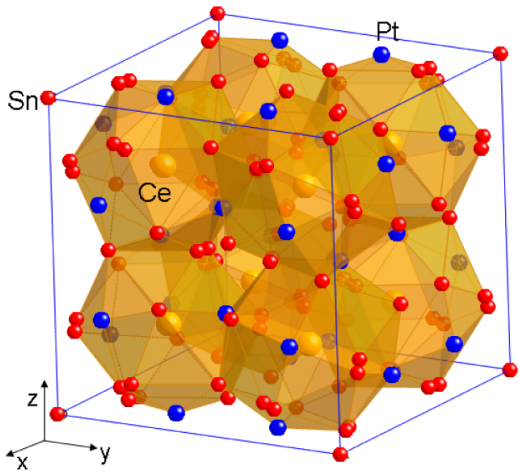

Figure 1. Three-dimensional representation of the crystal structure of $Ce_4Pt_{12}Sn_{25}$. Ce atoms are shown as faded larger spheres at the center of hexacapped-cuboctahedral cages of Sn and Pt atoms. See the text for details.

effective atoms around each Ce site in $Ce_4Pt_{12}Sn_{25}$ might be expected to lead to weaker f–p hybridization. Other materials with similarly large Ce–Ce distance (∼5.6 Å) include $CeNi_9X_4$ (X = Si, Ge). These compounds have strong hybridization between Ce-4f and conduction electrons from Ni and X ions, like Ce-skutterudites, where this hybridization dominates over the RKKY interaction due to large distances between Ce ions and leads to single-ion Kondo behavior [9].

The magnetic susceptibility, $\chi = M/H$, as a function of temperature, plotted in figure 2(a), appears to follow a Curie–Weiss law above 250 K with an effective moment of 2.2 μ_B/Ce, which is smaller than expected (2.54 μ_B/Ce) for the full Hund's rule degeneracy of Ce^{3+}. As discussed below, this smaller effective moment probably is the result of large crystal-field splitting of the $J = 5/2$ manifold. The Curie–Weiss temperature is negative with an absolute value of ∼6 K, suggesting weak antiferromagnetic exchange even at high temperatures. As shown in the inset of figure 2(a), the susceptibility again exhibits Curie–Weiss behavior below ∼4 K, but with a smaller effective moment (1.15 μ_B/Ce) and a smaller Curie–Weiss temperature of −0.4 K, which indicates very weak antiferromagnetic coupling of local moments to one another and to itinerant electrons. Field-dependent magnetization data at 2 K are plotted in figure 2(b). These data have been fitted by a Brillouin function, assuming a crystal-field doublet ground state with $g|J_z| = 0.675\ \mu_B$, which most likely implies a Γ_7 doublet ground state assuming $g = 6/7$. To track the magnetic response below 1.8 K, ac magnetic susceptibility was measured, with results presented in figure 2(c). Although somewhat noisy, these data increase with decreasing temperature below 2 K, as expected for a Curie–Weiss paramagnetic state, and exhibit a sharp kink at 0.19 K that is followed by a decrease at lower temperatures. This drop in susceptibility below 0.19 K rules out the ferromagnetic nature of this transition, but is consistent with an antiferromagnetic transition, as also indicated from the small, negative Weiss temperature inferred from the dc susceptibility.

Specific heat measurements support conclusions drawn from magnetic susceptibility and magnetization measure-

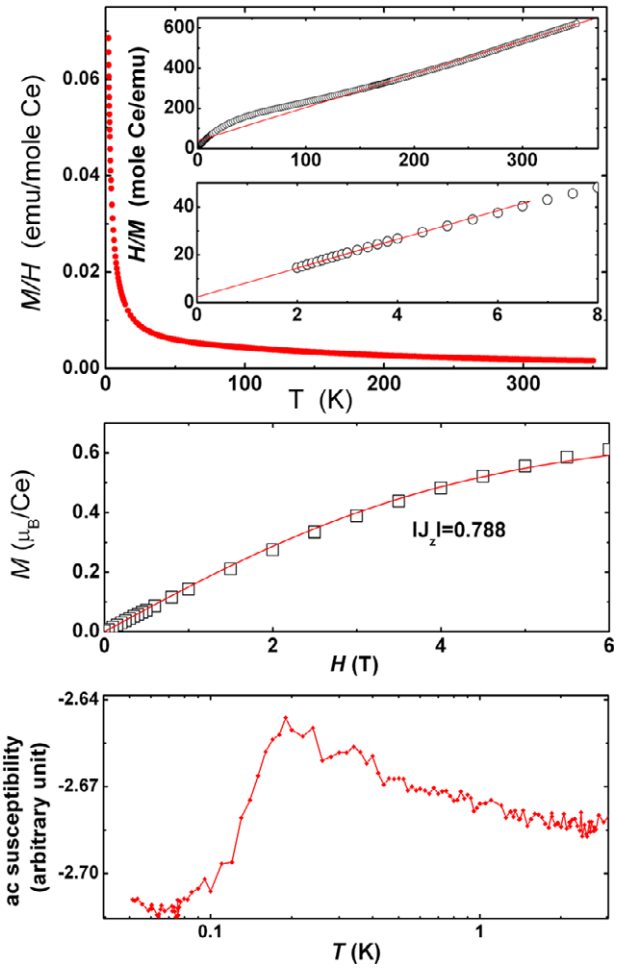

Figure 2. Magnetic susceptibility and magnetization of $Ce_4Pt_{12}Sn_{25}$. The upper panel is a plot of the dc susceptibility, measured in a field of 1 kOe, as a function of temperature. The inverse susceptibility over the whole temperature range and at low temperatures is shown in the insets. The middle panel is a plot of magnetization versus field measured at 2 K. The solid line is a fit to a Brillouin function as described in the text. The bottom panel shows ac magnetic susceptibility at low temperatures where there is a clear transition at 0.19 K.

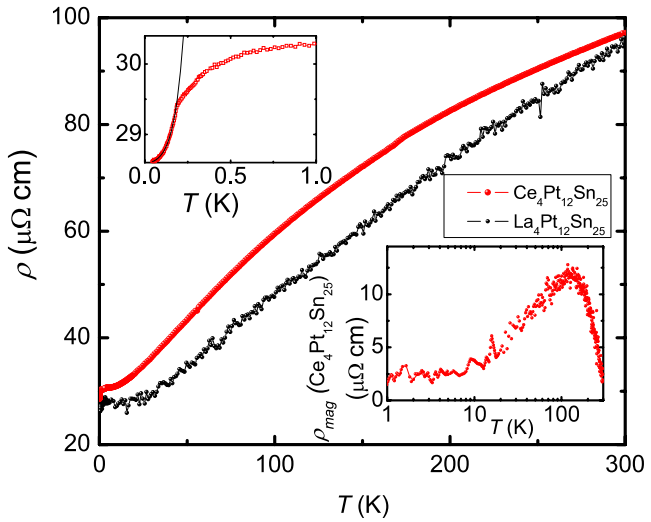

Figure 3. Magnetic contribution to the specific heat of $Ce_4Pt_{12}Sn_{25}$ obtained by subtracting the specific heat of non-magnetic $La_4Pt_{12}Sn_{25}$. The solid curve is a fit to the Schottky contributions from crystal-field excitations, as described in the text. The inset is a plot of C/T and magnetic entropy as a function of temperature. A second-order phase transition into an antiferromagnetic state is clear at 0.19 K. Below T_N, C/T is described well by $C/T = \gamma + AT^2$, with $\gamma = 0.45$ J mol^{-1} K^{-2} and $A = 1430$ J mol^{-1} K^{-3}, as discussed in the text. The dashed curve is calculated for a spin-1/2 Kondo impurity.

ments. Figure 3 shows the magnetic contribution C_{mag} to the specific heat of $Ce_4Pt_{12}Sn_{25}$, obtained by subtracting the specific heat of non-magnetic $La_4Pt_{12}Sn_{25}$ from the total specific heat of $Ce_4Pt_{12}Sn_{25}$. A broad peak in C_{mag} near 90 K is described reasonably well by Schottky contributions from two crystal-field doublets, separated from a ground state doublet by 199 and 247 K. The inverse susceptibility starts to deviate from linear behavior below about 250 K (see figure 2), consistent with this estimate of crystal-field excitation energies. The existence of crystal fields, as well as the high-temperature effective moment for $Ce_4Pt_{12}Sn_{25}$, suggests a well-localized Ce^{3+} state.

As shown in the inset of figure 3, there is a well-defined specific heat anomaly at 0.19 K, confirming the transition observed in the ac susceptibility. Below the transition, C/T follows a T^2 temperature dependence, which is expected for an antiferromagnetic magnon contribution. A magnetic field-induced decrease of the temperature at which an anomaly develops (data not shown) also supports the interpretation that the 0.19 K transition is into an antiferromagnetic state. Also shown in the inset is the evolution of magnetic entropy as a function of temperature. An entropy of $R \ln 2$ is recovered at ~2 K, consistent with antiferromagnetic order in a crystal-field doublet; however, only about 50% of $R \ln 2$ appears below T_N, with the remaining entropy reflected in the extremely large C/T that develops between ~2 K and T_N. Just above T_N, C/T reaches 14 J mol^{-1} K^{-2}, before it jumps to ~45 J mol^{-1} K^{-2} at 0.19 K. With the complex, three-dimensional structure of $Ce_4Pt_{12}Sn_{25}$, this large C/T extending from T_N to ~$10T_N$ cannot be due to critical fluctuations associated with the antiferromagnetic order. Numerical calculations for a 3D Heisenberg model, which fits reasonably well the shape of the feature associated with antiferromagnetic transition, do not completely account for the slow decrease of C/T above T_N observed experimentally; therefore, there exist effects above the transition other than just critical fluctuations due to a Heisenberg type exchange interaction [10].

One possible interpretation of the enhanced C/T above T_N is that it comes from the Kondo effect that also would lead to less than $R \ln 2$ entropy below T_N. For a spin-1/2 system, appropriate for a crystal-field doublet, $1/2R \ln 2$ develops on the temperature scale of approximately 80% of the Kondo-impurity temperature T_K. From the data in figure 3, this would imply an upper limit of $T_K \sim 0.26$ K. Using the model of Rajan [11], we calculate C/T for a $S = 1/2$ Kondo impurity with $T_K = 0.26$ K and show in the inset of figure 3 that the calculated temperature dependence does not describe the data. Indeed, the theoretical form alone cannot account for the data irrespective of the choice of T_K [11]. Moreover, the large specific heat above T_N does not increase with increasing

magnetic field until the magnetic transition is fully suppressed, which is contrary to expectations of Kondo-impurity physics. A fit to the specific heat below T_N gives a substantial T-linear term, $C = \gamma T$ where $\gamma \approx 0.45(\pm 0.24)$ J mol^{-1} K^{-2}. This value of γ is an upper limit, and its precise value is subject to some uncertainty because of experimental constraints imposed by the huge value of C/T at T_N, which is at least 100 times larger. Irrespective of its precise value, from our experiments, it is not possible to determine whether this T-linear term reflects the presence of Kondo-derived heavy quasiparticles or whether it has some other origin. We return to this in a discussion of the electrical resistivity.

With a substantial role of the Kondo effect in question, we consider other sources for such a large specific heat over a protracted temperature range above T_N. Intrinsic disorder from shared Sn3 and Sn3′ sites might play a role, but the sharp jump in specific heat at T_N does not support this possibility. Alternatively, it could be that the Ce moment is geometrically frustrated by the three-fold point symmetry of the Ce site. With this frustration-prone symmetry and Ce's coordination by six nearest and 12 next nearest neighbors, the coupling between nearest and next nearest neighbors could lead to frustration that is relieved only below T_N. In this scenario, however, we might expect T_N to be much less than the low-temperature Curie–Weiss scale, and the Curie–Weiss scale to be on the order of 2 K or higher (where C/T starts to grow dramatically), but neither of these conditions is observed. Yet another possibility is that the increase in C/T below 2 K is due to the development of short-range correlations among the Ce moments; however, why correlations should develop on a scale ten times T_N in this cubic compound is not obvious.

Figure 4 shows the temperature dependence of the electrical resistivity of $Ce_4Pt_{12}Sn_{25}$ and $La_4Pt_{12}Sn_{25}$. The resistivity is metallic and comparable for both compounds over the entire temperature range, and the ratio of resistivities at 300 and 2 K (RRR) is about 2.5–3.8, depending on the sample. The small RRR may be a consequence of structural disorder in Sn3 sites as discussed earlier. We note a barely detectable kink in the resistivity of $Ce_4Pt_{12}Sn_{25}$ near 170 K, where there also is a weak anomaly in specific heat but no feature in magnetic susceptibility. We tentatively attribute this kink to a still unknown change in crystal structure.

The magnetic resistivity of $Ce_4Pt_{12}Sn_{25}$, obtained by subtracting the resistivity of $La_4Pt_{12}Sn_{25}$, is presented in the lower inset of figure 4. A maximum in the magnetic resistivity near 120 K is consistent with scattering off excited crystal-field levels, possibly combined with some Kondo-like scattering in the excited levels [12], but there is no logarithmic dependence or a resistivity maximum at lower temperatures. The absence at lower temperatures of these characteristic signatures for Kondo-lattice behavior indicates that a Kondo effect, if present at low temperatures, should have a temperature scale on the order of T_N or lower. On the other hand, as shown in the upper inset of figure 4, the resistivity of $Ce_4Pt_{12}Sn_{25}$ below T_N is well-described by $\rho(T) = \rho_0 + AT^2 + BT^5$. The T^5 term is typical of scattering by antiferromagnetic spin waves, and the large T^2 coefficient, $A = 11\ \mu\Omega$ cm K^{-2}, is characteristic of heavy-fermion behavior in a Kondo lattice. In the Néel state,

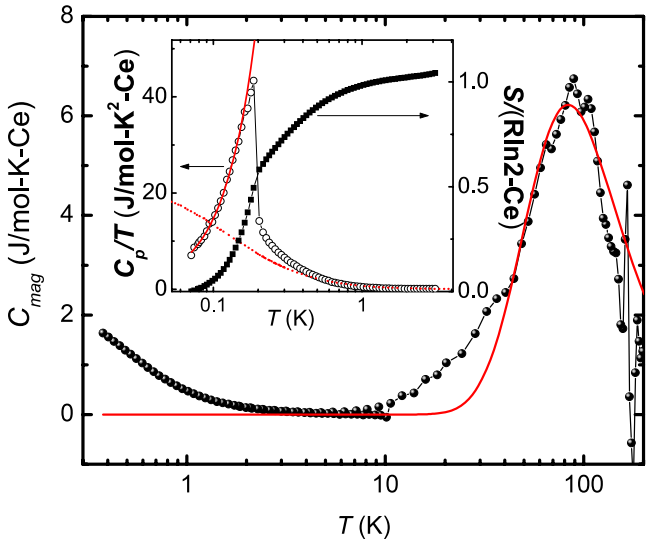

Figure 4. Electrical resistivity of $Ce_4Pt_{12}Sn_{25}$ (upper curve) and $La_4Pt_{12}Sn_{25}$ (lower curve) versus temperature. The upper inset shows the resistivity of $Ce_4Pt_{12}Sn_{25}$ near and above T_N. Below T_N, $\rho(T) = 28.6 + 11T^2 + 10\,560T^5$ $\mu\Omega$ cm. These temperature dependences are discussed in the text. Below ∼1 K, $\rho(T)$ decreases as T_N is approached. The lower inset shows the magnetic contribution to the resistivity of $Ce_4Pt_{12}Sn_{25}$, obtained by subtracting the resistivity of $La_4Pt_{12}Sn_{25}$. The peak in magnetic resistivity around 120 K is consistent with crystal-field effects in the presence of Kondo scattering, which causes a maximum in resistivity at roughly half of the crystal-field gap [12]. Note the absence of a logarithmic increase or a resistivity maximum below 120 K.

the ratio A/γ^2 is $>5 \times 10^{-5}$ $\mu\Omega$ cm (K mol mJ^{-1})^2, a value at least five times larger than the typical Kadowaki–Woods ratio found in Ce-based heavy-fermion systems [13]. In part, an enhanced Kadowaki–Woods ratio could arise from the small Fermi momentum of $Ce_4Pt_{12}Sn_{25}$, discussed below, but being inconclusive, it still leaves open the question of whether A and γ reflect heavy-fermion character.

There is no T^2 dependence to the resistivity above T_N; on the contrary, the resistivity decreases weakly and sublinearly with decreasing temperature below ∼1 K, as shown in the upper inset of figure 4. The temperature of the onset of the decreasing resistivity correlates with the beginning of the development of the large C/T above T_N. A reasonable interpretation of this relationship is that the decrease in $\rho(T)$ reflects a decrease in spin-disorder scattering due to the development of antiferromagnetic correlations among Ce moments that, in turn, are responsible for the increasing C/T as T_N is approached. Though neither frustration, Kondo correlations, nor antiferromagnetic correlations can by itself explain all experimental observations, we suggest a combination of a small magnetic exchange between Ce moments, between Ce moments and spins of itinerant electrons, and weak frustration is responsible for the extended temperature range over which these magnetic correlations persist.

We can estimate the scale of the magnetic exchange in $Ce_4Pt_{12}Sn_{25}$ as follows. From the discussion above, we assume that the Kondo-impurity scale is 0.26 K or less. This scale

is given by $T_K \approx [1/N_0]\exp(-1/(2JN_0))$, where N_0 is the unrenormalized density of electronic states that we obtain from the Sommerfeld coefficient $\gamma = 5$ mJ mol^{-1} K^{-2} of isoelectronic, non-magnetic $La_4Pt_{12}Sn_{25}$. Assuming $T_K = 0.26$ K, this expression gives $N_0J \leqslant 0.05$, which, indeed, puts $Ce_4Pt_{12}Sn_{25}$ in the very small J-limit of the Doniach model [14]. Further, a small RKKY scale, and hence T_N, in $Ce_4Pt_{12}Sn_{25}$ is due in part to its small Fermi momentum. Again using free electron relations, we estimate $k_F \approx 0.09$ Å^{-1} from the Sommerfeld coefficient of $La_4Pt_{12}Sn_{25}$. With a Ce–Ce spacing of $d = 6.14$ Å in $Ce_4Pt_{12}Sn_{25}$, $2k_Fd$ is somewhat smaller than $\pi/2$, where an oscillation in the RKKY interaction crosses zero. This estimate of $2k_Fd$ would imply that RKKY exchange in $Ce_4Pt_{12}Sn_{25}$ should be weakly ferromagnetic, but given the crudeness of our estimate, it is not inconsistent with a very small RKKY exchange and the small T_N that is observed.

We also can compare T_K estimated above with a molecular field calculation for a spin-1/2 resonant level model [15]. With the experimentally observed specific heat jump ($\Delta C_{mag} \sim 5.2$ J mol^{-1} K^{-2}) at T_N, this model gives a ratio of $T_K/T_N \sim 1$, which is consistent with our previous estimates and the expectation of small Kondo and magnetic interaction energy scales.

4. Summary

In summary, $Ce_4Pt_{12}Sn_{25}$ appears to be one of the few examples of a very small-J Kondo-lattice system. Most interesting is the very large C/T that develops above T_N and that represents 50% of $R\ln 2$ entropy at low temperatures. The origin of this large C/T does not have an obvious simple explanation nor is it clear that this is characteristic of all Kondo-lattices in the small J-limit. This behavior is not found in compounds with similar but non-frustrated structures, such as skutterudites. On the basis of electrical resistivity, specific heat, and magnetic susceptibility measurements, however, we suggest that it arises from the interplay among weak frustration, the development of short-range magnetic correlations, and a small magnetic exchange interaction between Ce moments and between Ce moments and spins of itinerant electrons. Neutron scattering and nuclear magnetic resonance (NMR) studies would be useful in resolving this interplay. We also find evidence for a structural transition near 170 K that might influence the interplay.

Acknowledgments

This work was supported by NSF-DMR 0854781 and NSF-DMR 0433560 (HL and ZF), NSF-DMR 0802478(PCH and MBM), and DMR-0600742(CLC and SMK). Work at Los Alamos was performed under the auspices of the US Department of Energy/Office of Science.

References

[1] Stewart G R 1984 *Rev. Mod. Phys.* **56** 755
[2] Stewart G R 2001 *Rev. Mod. Phys.* **73** 797
[3] Kondo J 1964 *Prog. Theor. Phys.* **32** 37
[4] Ruderman M A and Kittel C 1954 *Phys. Rev.* **96** 99
[5] Doniach S 1977 *Physica* B **91** 231
[6] Mathur N D, Grosche F M, Julian S R, Walker I R, Freye D M, Haselwimmer R K W and Lonzarich G G 1998 *Nature* **394** 39
Schroder A, Aeppli G, Coldea R, Adams M, Stockert O, von Lohneysen H, Cucher E, Ramazashivilli R and Coleman P 2000 *Nature* **407** 351
Park T, Ronning F, Yuan H Q, Salamon M B, Movshovich R, Sarrao J L and Thompson J D 2006 *Nature* **440** 76
[7] Chafik B, Idrissi El, Venturini G and Malaman B 1990 *Mater. Res. Bull.* **25** 807
[8] Aoki Y, Sugawara H, Hisatomo H and Sato H 2005 *J. Phys. Soc. Japan* **74** 209
[9] Sengupta K and Sampathkumaran E V 2006 *J. Phys.: Condens. Matter* **18** L115
Michor H, Adroja D T, Bauer E, Bewley R, Dobozanov D, Hillier A D, Hilscher G, Killer U, Koza M, Manalo S, Manuel P, Reissner M, Rogl P, Rotter M and Scheidt E-W 2006 *Physica* B **378–380** 640
[10] Kurita N *et al* 2010 in preparation
[11] Rajan V T 1983 *Phys. Rev. Lett.* **51** 308
Sacramento P D and Schlottmann P 1989 *Phys. Rev.* B **40** 431
[12] Cornut B and Coqblin B 1972 *Phys. Rev.* B **5** 4541
[13] Tsujii N, Kontani H and Yoshimura K 2005 *Phys. Rev. Lett.* **94** 077201
[14] Yang Y, Fisk Z, Lee H, Thompson J D and Pines D 2008 *Nature* **454** 611
[15] Besnus M J, Braghta A, Hamdaoui N and Meyer A 1992 *J. Magn. Magn. Mater.* **104–107** 1385